Structural Engineering and Mechanics, Vol. 21, No. 5 (2005) 591-620
DOI: http://dx.doi.org/10.12989/sem.2005.21.5.591

Mechanical properties of thin-walled composite beams of generic open and closed sections

S. Rajasekaran†

PSG College of Technology, Coimbatore, 641004, Tamilnadu, India

(Received December 8, 2004, Accepted September 2, 2005)

Abstract. A general analytical model for thin-walled composite beams with an arbitrary open/(or/and) closed cross section and arbitrary laminate stacking sequence i.e., symmetric, anti-symmetric as well as un-symmetric with respect to the mid plane of the laminate, is developed in the first paper. All the mechanical properties, mechanical centre of gravity and mechanical shear centre of the cross section are defined in the function of the geometry and the material properties of the section. A program "fungen" and "clprop" are developed in Fortran to compute all the mechanical properties and tested for various isotropic sections first and compared with the available results. The locations of mechanical centre of gravity and mechanical shear centre are given with respect to the fibre angle variation in composite beams. Variations of bending and torsional stiffness are shown to vary with respect to the fibre angle orientations.

Key words: FRP (Fibre reinforced plastics); thin-walled composite; open section; mechanical centre of gravity; mechanical shear centre.

1. Introduction

FRP has been increasingly used over the past few decades in a variety of structures that require high ratio of stiffness and strength to weight ratios. Recent applications in the construction industry have shown the structural and cost efficiency of FRP structural shapes such as thin-walled open and closed sections. Another primary advantage of composites is tailorability. Material and structural properties can be designed to fit each application. The designer can choose from a variety of fibre and resin systems and fibre orientations to achieve the optimal performance of the structure.

Thin-walled composite beams are extensively used as truss members, stiffeners, rotor blade spars, columns and many other structural elements. In the case of thin-walled composite beams, the designer is able to optimize not only the cross sectional shape but also the material itself to achieve for example, high bending, torsion and axial stiffness (or some combination thereof).

Many researchers like Vlasov (1961), Gjelsvik (1981), Murray (1984), Murray and Rajasekaran (1975), Rajasekaran and Padmanabhan (1989), Rajasekaran (1994), Taufik *et al.* (1999), Wu and Sun (1992) have studied isotropic thin-walled members of open cross section. For an-isotropic composite materials, however, the geometric properties used in classical isotropic beam theory such as area, first moment of area, centre of gravity and shear centre etc. are no longer used because the

† Professor of Infrastructure Engineering, E-mail: sekaran@hotmail.com

variability of material properties in the cross section. Instead, mechanical properties such as axial stiffness, mechanical first moment of area, mechanical centre of gravity and mechanical shear centre should be defined to incorporate both geometry and the material properties. Bauld and Tzeng (1984) extended Vlasov's theory to thin-walled beams to symmetric fibre reinforced laminates to develop the linear and nonlinear theories for the bending and twisting of thin-walled composite beams. Lee (2000) has discussed the centre of gravity and shear centre of thin-walled open section composite beams. It appears that the general definition of centre of gravity and shear centre of laminated open and closed symmetric, anti-symmetric and un-symmetric beams with general configuration has not been treated in open literature. Wagner and Gruttmann (2002) analysed thin-walled isotropic composite beams for flexural stresses using displacement method.

Already Murray and Rajasekaran (1975) have developed a technique for formulating the beam equations reported in Theory of Beam-Columns (Chen and Atsuto 1977, Rajasekaran and Padmanabhan 1989) for curved beams and Rajasekaran (1994) for tapered thin-walled beams of generic open section. In similar lines, in the present study, a general analytical model for thin-walled laminated composite beams with an arbitrary open or closed cross section and arbitrary laminate sequence in un-symmetric, symmetric and anti-symmetric with respect to mid plane laminate is developed. The variation of mechanical properties with respect to fibre orientation is also given.

2. Kinematics

The present work is aimed at developing a geometrically non-linear theory valid for composite beams of open/closed (with one or more cells)/combination of open and closed sections. To be specific, the theory accounts for anisotropy, constrained warping and bending stiffness of the beam

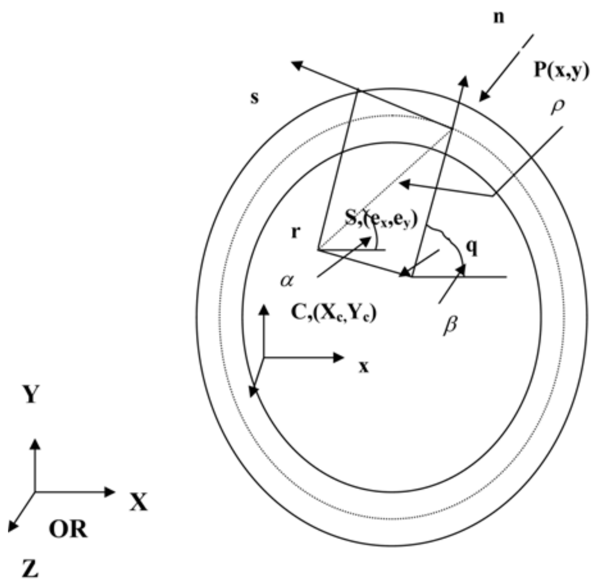

Fig. 1 Definitions of coordinates in thin-walled section

as well. Theoretical developments presented in this paper require four sets of coordinate systems, which are mutually inter-related. The first coordinate system is the orthogonal Cartesian system (X, Y, Z) passing through any reference point 'OR' for which the X and Y axes lie in the plane of the cross section and Z axis parallel to the longitudinal axis of the beam. The second coordinate system is the orthogonal Cartesian system (x, y, z) passing through the point C (X_C, Y_C). The third coordinate system is the local plate coordinate system (n, s, z) as shown in Fig. 1 where 'n' axis is normal to the middle surface of a plate element, the 's' axis is the tangent to the middle surface and is directed along the contour line of the cross section. The (n, s, z) and (X, Y, Z) coordinate system are related through an angle of orientation 'β' as defined in Fig. 1. 'β' is measured positive in the anti-clockwise direction and is the angle of orientation of 'n' axis with respect to 'X' axis at any point 'P'. The fourth coordinate set is the contour coordinate 's' along the profile of the section with its origin at any point 'O' on the profile of the cross section. Point 'S' (e_X, e_Y) is called 'pole axis' in this paper. The wall thickness and the material properties are assumed to be invariant along the length of the beam but can vary with respect to 's'. The theory developed in this paper is based on the following hypotheses.

3. Assumptions made

1. The flexure displacement 'u' and 'v' in X and Y directions respectively and the twist 'ϕ' of the cross section are small.
2. The axial displacement 'w' is much smaller than 'u' and 'v' so that the products of the derivatives of 'w' can be neglected in the strain displacement relation.
3. The projection of the cross section on a plane normal to the Z-axis does not distort during deformation.
4. The torsional shear strain 'γ_{sz}' on the middle surface of the beam wall is zero for an open contour while it corresponds to the constant shear flow (with respect to 's') for a closed contour.
5. Strains are small so that a linear constitutive law can be used to relate the second Piola-Kirchhoff's stress tensor to Green's strain tensor.
6. The ratio of wall thickness to the radius of curvature at any point of the beam wall is small compared to unity so that it can be neglected in the expression of the strains. It should be noted that this is actually exact for cross sections composed of linear segments.
7. The shell force and moment resultants corresponding to the circumferential normal stress 'σ_{ss}' and the force resultant corresponding to 'γ_{ns}' are negligibly small.
8. 'σ_{nn}' can be neglected when deriving the stress-strain law of any layer of the beam wall.
9. Kichhoff-Love assumption in classical theory remains valid for laminated composite thin-walled beams.

4. Strains and displacement

The coordinates of 'P' on the contour of thin-walled cross section with respect to 'x, y' axes passing through 'C' are (x, y) and the coordinates of 'S' with respect to x, y axes are (e_x, e_y). Consider the beam twists by an angle of 'ϕ' with respect to 'z' axis passing through 'S' (See Fig. 2).

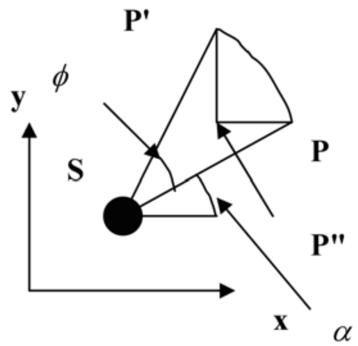

Fig. 2 Rotation about S axis

The displacement due to rotation 'ϕ' of point 'P' in 'x' direction is given as

$$PP'' = \rho\cos(\phi + \alpha) - \rho\cos\alpha \tag{1}$$

For small angle of twist $\cos\phi = 1$; and $\sin\phi = \phi$;

$$PP'' = -(y - e_y)\phi \tag{2}$$

The displacement in 'y' direction of point 'P' due to twist is given as

$$P'P'' = \rho\sin(\alpha + \phi) - \rho\sin\alpha \tag{3a}$$

$$P'P'' = (x - e_x)\phi \tag{3b}$$

In Eqs. (1) and (3a) ρ and α denote the distance 'SP' and the angle 'SP' makes with x-axis. In addition to twist if the displacements of 'S' in x and y directions are also added, we get the displacements of 'P' in x and y directions as

$$u = u_S - (y - e_y)\phi \tag{4a}$$

$$v = v_S + (x - e_x)\phi \tag{4b}$$

The relationship between (n, s, z) and (x, y, z) coordinate system can be written as

$$\begin{Bmatrix} \bar{i} \\ \bar{j} \\ \bar{k} \end{Bmatrix} = \begin{bmatrix} \cos\beta & -\sin\beta & 0 \\ \sin\beta & \cos\beta & 0 \\ 0 & 0 & 0 \end{bmatrix} \begin{Bmatrix} \bar{e}_n \\ \bar{e}_s \\ \bar{k} \end{Bmatrix} \tag{5a}$$

$$\begin{Bmatrix} \bar{e}_n \\ \bar{e}_s \\ \bar{k} \end{Bmatrix} = \begin{bmatrix} \cos\beta & \sin\beta & 0 \\ -\sin\beta & \cos\beta & 0 \\ 0 & 0 & 1 \end{bmatrix} \begin{Bmatrix} \bar{i} \\ \bar{j} \\ \bar{k} \end{Bmatrix} \tag{5b}$$

where $\bar{i}, \bar{j}, \bar{k}, \bar{e}_n, \bar{e}_s$ are unit vectors in the x, y, z and n and s directions respectively.

The displacements at point 'P' in 'n' and 's' directions $\bar{u}$, $\bar{v}$ are given as

$$\begin{Bmatrix} \bar{u} \\ \bar{v} \end{Bmatrix} = \begin{bmatrix} \cos\beta & \sin\beta \\ -\sin\beta & \cos\beta \end{bmatrix} \begin{Bmatrix} u_s - (y - e_y)\phi \\ v_s + (x - e_x)\phi \end{Bmatrix} \tag{6}$$

$$\bar{u} = u_s \cos\beta + v_s \sin\beta + q\phi \tag{7a}$$

$$\bar{v} = -u_s \sin\beta + v_s \cos\beta + r\phi \tag{7b}$$

where 'r' and 'q' are the perpendicular distances from 'S' to 's' and 'n' axes respectively at the point 'P'.

The strain displacement relations for the three components ε_{xx}, ε_{yy} and γ_{xy} of Green's strain tensor, with due regard to assumption 2 are given by

$$\varepsilon_{xx} = u_{,x} + \frac{1}{2}(u_{,x}^2 + v_{,x}^2) \tag{8a}$$

$$\varepsilon_{yy} = v_{,y} + \frac{1}{2}(u_{,y}^2 + v_{,y}^2) \tag{8b}$$

$$\gamma_{xy} = u_{,y} + v_{,x} + \frac{1}{2}(u_{,x}u_{,y} + v_{,x}v_{,y}) \tag{8c}$$

where 'ε' is the normal strain and 'γ' is the shear strain. In Eq. (8) a subscript comma denotes differentiation. Substituting Eq. (4) in Eq. (8) yields zero for all the three strains thus verifying cross sectional non-deformability. This also implies that assumption 2 and 3 are mutually compatible.

The warping displacement (axial displacement in 'z' direction) is obtained by considering the shear strains 'γ_{sz}' and 'γ_{nz}'. Consider $h(s)$ as the thickness of the wall consisting of many layers of composite laminates and $\bar{N}_{sz}(z, n)$, $\bar{G}_{sz}(s)$ be the torsional shear flow and the effective in-plane shear stiffness of the laminate (to be defined later) respectively with reference to a closed contour. Then the shear strain 'γ_{sz}' at any point of the mid surface of the contour is given by

$$\gamma_{sz}^* = \bar{v}_{,z}^* + w_{,s}^* + \frac{1}{2}(\bar{v}_{,s}^* \bar{v}_{,z}^* + w_{,s}^* w_{,z}^*) \tag{9}$$

$$\bar{v}_{,z}^* + w_{,s}^* = 0 + \delta_c \frac{\bar{N}_{sz}(z, n)}{h(s)\bar{G}_{sz}(s)} \tag{10}$$

In Eq. (10) 'δ_c' is a tracer as defined by Bhaskar and Librescu (1995) for indicating a closed cross section where '$\delta_c = 1$ or 0' depending on whether the cross section is closed or open. For the sake of clarity all the mid surface quantities are indicated by asterisk (*) whenever applicable.

In Eq. (10) by virtue of assumption 6 $\bar{v}_{,s}^* = 0$ since the cross section is made up of linear segments and the product term $w_{,s}^*$, $w_{,z}^*$ is small and neglected. Hence from Eq. (10) we can write

$$w_{,s}^* = -\bar{v}_{,z}^* + \delta_c \frac{\bar{N}_{sz}}{h\bar{G}_{sz}} \tag{11}$$

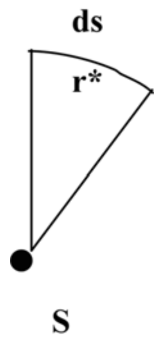

Fig. 3 Definition of sectorial coordinate

Substituting for $\bar{v}^*_{,z}$ from Eq. (7b), we get

$$w^*_{,s} = -u_{s,z}\sin\beta + v_{s,z}\cos\beta + r^*\phi_{,z} + \delta_c \frac{\bar{N}_{sz}}{h\bar{G}_{sz}} \tag{12}$$

or

$$w^*_{,s} = -\left(u_s'\frac{dx}{ds} + v_s'\frac{dy}{ds} + r^*\phi'\right) + \delta_c \frac{\bar{N}_{sz}}{h\bar{G}_{sz}} \tag{13}$$

where u_s' denotes $\dfrac{du_s}{dz}$.

Integrating both sides of Eq. (13) with respect to 's', we get

$$w^* - w_0^* = -u_s'(x^* - x_0^*) - v_s'(y^* - y_0^*) + \phi'(\omega^* - \omega_0^*) + \delta_c \int_0^s \frac{\bar{N}_{sz}}{h\bar{G}_{sz}} ds \tag{14}$$

where ω^* is the sectorial coordinate given by twice sectorial area i.e., (see Fig. 3) as

$$\omega^* = -\int r^* ds \tag{15}$$

In case of closed contour (with one cell) $\bar{N}_{sz}$ is an indeterminate quantity and can be obtained from the following contour integral equation for the cell as

$$\oint \frac{dw^*}{ds} ds = 0 \tag{16}$$

From Eq. (13), we get

$$\phi' \oint r^* ds = \oint \frac{\bar{N}_{sz}}{h\bar{G}_{sz}} ds \tag{17}$$

or

$$\bar{N}_{sz} = \phi' \frac{\oint r^* ds}{\oint \dfrac{ds}{h\bar{G}_{sz}}} \tag{18}$$

In case of multi-cells $(\overline{N}_{sz})_i$ is the indeterminate shear flow in each cell and there will be unknown shear flows equal to the number of cells and can be found out by solving simultaneous equations, which will be discussed in the later part of the paper.

Substituting Eq. (18) in Eq. (14), we get

$$w^* = \{w_0^* + x_0^* u_s' + y_0^* v_s' - \omega_0^* \phi'\} - x^* u_s' + y^* v_s' + \phi' \left(\omega^* + \delta_c \frac{\oint r^* ds \int_0^s \frac{ds}{h\overline{G}_{sz}}}{\oint \frac{ds}{h\overline{G}_{sz}}} \right) \tag{19}$$

Defining

$$w_c = w_0^* + x_0^* u_s' + y_0^* v_s' - \omega_0^* \phi' \tag{20}$$

$$\psi = \frac{1}{h\overline{G}_{sz}} \frac{\oint r^* ds}{\oint \frac{ds}{h\overline{G}_{sz}}} \tag{21}$$

Axial displacement at mid line of the contour is given as

$$w^* = w_c - x^* u_s' - y^* v_s' + \left(\omega^* + \delta_c \int_0^s \psi ds \right) \phi' \tag{22}$$

or

$$w^* = w_c - x^* u_s' - y^* v_s' + \overline{\omega}^* \phi' \tag{23}$$

where $\overline{\omega}^*$ or simply $\overline{\omega}$ is called modified warping coordinate valid for both open and closed sections given by

$$\overline{\omega} = \overline{\omega}^* = \omega^* + \delta_c \int_0^s \psi ds \tag{24}$$

In Eq. (23) we represent a measure of the overall 'z' displacement of the cross section. It should be mentioned that in the present theory ϕ' turns out to be a function of 'z' and not a constant as in St-Venant's theory and hence presents model accounts for non-uniform torsion due to restrained warping.

The displacements u, v, w at any generic point on the projected cross section are given by (see Fig. 4) mid surface displacements u^*, v^* and w^* by assumption 9 as

$$u(s, z, n) = \overline{u}^*(s, z) \tag{25a}$$

$$v(s, z, n) = \overline{v}^*(s, z) - n\frac{\partial \overline{u}^*(s, z)}{\partial s} \tag{25b}$$

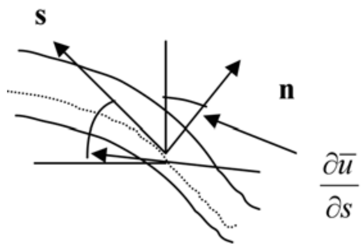

Fig. 4 Definition of slope

$$w(s, z, n) = w^*(s, z) - n\frac{\partial \bar{u}^*(s, z)}{\partial z} \tag{25c}$$

The strains associated with small displacement theory of elasticity at mid surface are given by

$$\bar{\varepsilon}_n^* = \frac{\partial \bar{u}^*}{\partial n} = 0; \quad \bar{\varepsilon}_s^* = \frac{\partial \bar{v}^*}{\partial s}; \quad \bar{\varepsilon}_z^* = \frac{\partial w^*}{\partial z} \tag{26}$$

$$\bar{\gamma}_{sz}^* = 0 + \delta_c \frac{\bar{N}_{sz}}{h\bar{G}_{sz}}\phi' \tag{27}$$

The strains at any point are given by

$$\varepsilon_s = \varepsilon_s^* + n\bar{\kappa}_s \tag{28a}$$

$$\varepsilon_z = \varepsilon_z^* + n\bar{\kappa}_z \tag{28b}$$

$$\gamma_{sz} = \delta_c \frac{\bar{N}_{sz}}{h\bar{G}_{sz}}\phi' + n\bar{\kappa}_{sz} \tag{28c}$$

where

$$\bar{\kappa}_s = -\frac{\partial^2 \bar{u}^*}{\partial s^2}; \quad \bar{\kappa}_z = -2\frac{\partial^2 \bar{u}}{\partial s\,\partial z}; \quad \bar{\kappa}_{sz} = -2\frac{\partial^2 \bar{u}^*}{\partial z\,\partial z} \tag{29}$$

All other strains are identically zero. In Eq. (29), $\bar{\varepsilon}_s^*$ and $\bar{\kappa}_s$ are assumed to be zero and $\bar{\varepsilon}_z^*$, $\bar{\kappa}_z$ and $\bar{\kappa}_{sz}$ are mid surface axial strain and bi-axial curvatures of the shell respectively. The above shell strains can be converted to beam strain components. By substituting Eq. (7) and Eq. (23) in Eq. (29), we get

$$\bar{\varepsilon}_z^* = (w^{*\prime}) = w_c' - x^* u_s'' - y^* v_s'' + \bar{\omega}\phi'' \tag{30}$$

and

$$\varepsilon_z = \bar{\varepsilon}_z^* + n\bar{\kappa}_z = w_c' - x^* u_s'' - y^* v_s'' + \bar{\omega}\phi'' - n\bar{u}^{*\prime} \tag{31}$$

or

$$\varepsilon_z = w_c' - (x^* + n\cos\beta)u_s'' - (y^* + n\sin\beta)v_s'' + (\overline{\omega} - nq)\phi'' \tag{32}$$

where prime (’) denotes differential with respect to ‘z’ and double prime (’’) denotes double differential with respect to ‘z’.

The shear strain γ_{sz} can be written as

$$\gamma_{sz} = \delta_c \frac{\overline{N}_{sz}}{h\overline{G}_{sz}}\phi' + n\left(-2\frac{\partial^2 \overline{u}^*}{\partial s\,\partial z}\right) \tag{33}$$

$$= (\delta_c \psi - 2n)\phi' \tag{34}$$

Hence normal strain ε_z and shear strain γ_{sz} can be written in terms of displacements as

$$\begin{Bmatrix} \varepsilon_z \\ \gamma_{sz} \end{Bmatrix} = \begin{bmatrix} 1 & (x^* + n\cos\beta) & (y^* + n\sin\beta) & (\overline{\omega} - nq) & 0 \\ 0 & 0 & 0 & 0 & (\delta_c \psi - 2n) \end{bmatrix} \begin{Bmatrix} w_c' \\ -u_s'' \\ -v_s'' \\ \phi'' \\ \phi' \end{Bmatrix} \tag{35}$$

or

$$\{\varepsilon\} = [B]\{q\} \tag{36}$$

5. Constitutive equations

Thin-walled beam can be considered to be made up of thin plate elements as shown in Fig. 5 of total thickness ‘h’ consisting of ‘n’ orthotropic layers with the principal natural coordinates ‘L, T, Z’ directions with Z-axis (z-axis) taken positive upward at middle plane (see Fig. 6). The following assumptions are made.

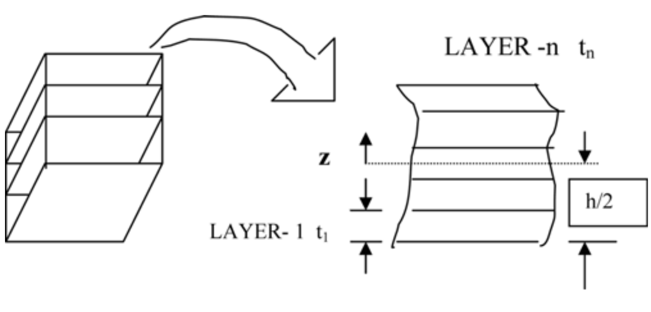

Fig. 5 Coordinate system and layer numbering

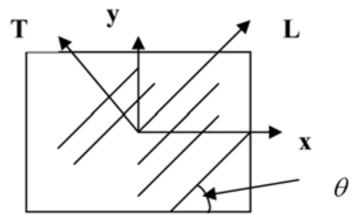

Fig. 6 x, y, L, T system

1. The layers are perfectly bonded together.
2. The material of the layer is linearly elastic and has two planes of natural symmetry.
3. Each layer is of uniform thickness.
4. The transverse shear stresses on top and bottom surfaces of the laminate are zero.
5. Kirchhoff's assumption holds good.
6. The transverse normal does not suffer any elongation.
7. The transverse normal rotates such that it remains perpendicular to the mid surface after deformation.

Taking a laminate shown in Fig. 6 and using the notations commonly adopted in composite literature given by Kaw (1997), one can give stresses in X, Y coordinate directions in terms of principal coordinates namely LT as

$$\begin{Bmatrix} \sigma_{xx} \\ \sigma_{yy} \\ \sigma_{xy} \end{Bmatrix} = [T] \begin{Bmatrix} \sigma_{LL} \\ \sigma_{TT} \\ \sigma_{LT} \end{Bmatrix} \tag{37}$$

where $[T]$ is the stress transformation matrix. Using the constitutive law, the stress strain relationship in LT system can be written as

$$\begin{Bmatrix} \sigma_{LL} \\ \sigma_{TT} \\ \sigma_{LT} \end{Bmatrix} = \begin{bmatrix} Q_{11} & Q_{12} & Q_{16} \\ Q_{21} & Q_{22} & Q_{26} \\ Q_{61} & Q_{62} & Q_{66} \end{bmatrix} \begin{Bmatrix} \varepsilon_L \\ \varepsilon_T \\ \gamma_{LT} \end{Bmatrix} \tag{38}$$

where

$$[Q] = \frac{1}{(1 - \nu_{LT}\nu_{TL})} \begin{bmatrix} E_L & \nu_{LT}E_T & 0 \\ \nu_{TL}E_L & E_T & 0 \\ 0 & 0 & G_{LT}(1 - \nu_{LT}\nu_{TL}) \end{bmatrix} \tag{39}$$

Using the transformation law, the constitutive matrix in XY system is obtained as

$$\begin{Bmatrix} \sigma_{XX} \\ \sigma_{YY} \\ \sigma_{XY} \end{Bmatrix} = \begin{bmatrix} S_{11} & S_{12} & S_{16} \\ S_{21} & S_{22} & S_{26} \\ S_{61} & S_{62} & S_{66} \end{bmatrix} \begin{Bmatrix} \varepsilon_X \\ \varepsilon_Y \\ \gamma_{XY} \end{Bmatrix} \tag{40}$$

or

$$[s] = [T][Q][T]^T \tag{41}$$

where

$$[T] = \begin{bmatrix} \cos^2\theta & \sin^2\theta & -\sin 2\theta \\ \sin^2\theta & \cos^2\theta & \sin 2\theta \\ \dfrac{\sin 2\theta}{2} & -\dfrac{\sin 2\theta}{2} & \cos 2\theta \end{bmatrix} \tag{42}$$

where 'θ' is the fibre orientation of laminate with respect to X axis of the plate. It should be noted that X axis of the plate (lamina) corresponds to z (Z) axis of the beam and θ is the fibre orientation with respect of 'z' axis of the beam.

The constitutive equation of the 'k'th orthotropic lamina in the beam coordinate system is given as

$$\{\sigma\} = \begin{Bmatrix} \sigma_z \\ \tau_{sz} \end{Bmatrix}^k = \begin{bmatrix} S_{11} & S_{16} \\ S_{61} & S_{66} \end{bmatrix} \begin{Bmatrix} \varepsilon_z \\ \gamma_{sz} \end{Bmatrix} \tag{43}$$

It is seen from Eq. (43) that σ_z and τ_{sz} are the normal and shear stresses at any point of the thin-walled contour and they are same as σ_{XX} and σ_{XY} given in Eq. (41).

From Eq. (36) and using contra-gradient law, we get

$$\{Q\} = \int_A [B]^T \{\sigma\} dA \tag{44}$$

where $\{Q\}$ are the generalized forces corresponding to $\{q\}$ where

$$\langle q \rangle = \langle w_c' \;\; -u_s'' \;\; -v_s'' \;\; \phi'' \;\; \phi' \rangle \tag{45a}$$

$$\langle Q \rangle = \langle P \;\; M_y \;\; M_x \;\; M_\omega \;\; T \rangle \tag{45b}$$

where P = axial load; M_y, M_x = moments about y and x axes passing through 'C' and M_ω denotes warping moment (bi-moment as defined by Vlasov 1961) and T = Torsional moment. Hence generalized forces are written in terms of stresses as

$$\begin{Bmatrix} P \\ M_y \\ M_x \\ M_\omega \\ T \end{Bmatrix} = \sum_{k=1}^{n} \int [B]^T \begin{Bmatrix} \sigma_z \\ \tau_{sz} \end{Bmatrix} dnds \tag{46a}$$

or

$$\begin{Bmatrix} P \\ M_y \\ M_x \\ M_\omega \\ T \end{Bmatrix} = \left[\sum_{k=1}^{n} \int [B]^T \begin{bmatrix} S_{11} & S_{16} \\ S_{61} & S_{66} \end{bmatrix} [B] dnds\right] \begin{Bmatrix} w_c' \\ -u_s'' \\ -v_s'' \\ \phi'' \\ \phi' \end{Bmatrix} \tag{46b}$$

or

$$\begin{Bmatrix} P \\ M_y \\ M_x \\ M_\omega \\ T \end{Bmatrix} = \begin{bmatrix} E_{11} & E_{12} & E_{13} & E_{14} & E_{15} \\ E_{21} & E_{22} & E_{23} & E_{24} & E_{25} \\ E_{31} & E_{32} & E_{33} & E_{34} & E_{35} \\ E_{41} & E_{42} & E_{43} & E_{44} & E_{45} \\ E_{51} & E_{52} & E_{53} & E_{54} & E_{55} \end{bmatrix} \begin{Bmatrix} w_c' \\ -u_s'' \\ -v_s'' \\ \phi'' \\ \phi' \end{Bmatrix} \tag{47}$$

where E_{ij} is the mechanical stiffness of a thin-walled composite beam cross section and it is symmetric and defined by

$$E_{11} = \int A_{11} ds \tag{48a}$$

$$E_{12} = \int (A_{11} x^* + B_{11} \cos\beta) ds \tag{48b}$$

$$E_{13} = \int (A_{11} y^* + B_{11} \sin\beta) ds \tag{48c}$$

$$E_{14} = \int (A_{11} \overline{\omega} - B_{11} q) ds \tag{48d}$$

$$E_{15} = -2 \int B_{16} ds + \delta_c \int A_{16} \psi ds \tag{48e}$$

$$E_{22} = \int (A_{11} x^{*2} + 2B_{11} x^* \cos\beta + D_{11} \cos^2\beta) ds \tag{48f}$$

$$E_{23} = \int (A_{11} x^* y^* + B_{11}(x^* \sin\beta + y^* \cos\beta) + D_{11} \sin\beta \cos\beta) ds \tag{48g}$$

$$E_{24} = \int (A_{11} \overline{\omega} x^* - B_{11} q x^* + B_{11} \overline{\omega} \cos\beta - D_{11} q \cos\beta) ds \tag{48h}$$

$$E_{25} = -2 \int (B_{16} x^* + D_{16} \cos\beta) ds + \delta_c \int (A_{16} x^* \psi + B_{16} \psi \cos\beta) ds \tag{48i}$$

$$E_{33} = \int (A_{11} y^{*2} + 2B_{11} y^* \sin\beta + D_{11} \sin^2\beta) ds \tag{48j}$$

$$E_{34} = \int (A_{11} \overline{\omega} y^* - B_{11} q y^* + B_{11} \overline{\omega} \sin\beta - D_{11} q \sin\beta) ds \tag{48k}$$

$$E_{35} = -2 \int (B_{16} y^* + D_{16} \sin\beta) ds + \delta_c \int (A_{16} y^* \psi + B_{16} \psi \sin\beta) ds \tag{48l}$$

$$E_{44} = \int (A_{11} \overline{\omega}^2 - 2B_{11} q \overline{\omega} + D_{11} q^2) ds \tag{48m}$$

$$E_{35} = -2\int(B_{16}\overline{\omega} - D_{16}q)ds + \delta_c\int(A_{16}\overline{\omega}\psi - B_{16}\psi q)ds \tag{48n}$$

$$E_{55} = 4\int D_{66}ds + \delta_c[\int(A_{66}\psi^2 - 4B_{66}\psi)ds] \tag{48o}$$

A_{ij}, B_{ij}, D_{ij} matrices are extensional, coupling and bending stiffnesses respectively defined by

$$A_{ij}, B_{ij}, D_{ij} = \int S_{ij}(1, n, n^2)dn \tag{49}$$

and are explicitly given as

$$A_{ij} = \sum\int S_{ij}dn = \sum_{k=1}^{n} S_{ij}^{k}(z_{k+1} - z_k) \tag{50a}$$

$$B_{ij} = \sum\int S_{ij}ndn = \frac{1}{2}\sum_{k=1}^{n} S_{ij}^{k}(z_{k+1}^2 - z_k^2) \tag{50b}$$

$$D_{ij} = \sum\int S_{ij}n^2dn = \frac{1}{3}\sum_{k=1}^{n} S_{ij}^{k}(z_{k+1}^3 - z_k^3) \tag{50c}$$

Knowing the stress resultants, one can solve for generalized strains and curvatures as

$$\begin{Bmatrix} w_c' \\ -u_s'' \\ -v_s'' \\ \phi'' \\ \phi' \end{Bmatrix} = [E]^{-1}\begin{Bmatrix} P \\ M_y \\ M_x \\ W_\omega \\ T \end{Bmatrix} \tag{51}$$

One way of solving the five simultaneous equations represented by Eq. (47) would be to use the process of elimination. Another way is to get the matrix equivalent of a thin-walled beam by changing the axes of reference both in position and direction and the process is known as orthogonalization and it is possible because E matrix is symmetric. In Eq. (47) w_c', u_s'', v_z'', ϕ'', ϕ' appear in all the five equations and they are coupled. After orthogonalization each variable will appear in one and only one equation, i.e., the equations are uncoupled. When the reference axes are principal axes passing through mechanical Centroid, pole is chosen at mechanical Shear Centre and the origins of contour chosen at Sectorial Centroid $[E]$ and $[E]^{-1}$ are diagonal matrices.

6. Mechanical centroid

In Fig. 1 'C' is a mechanical centroid if $E_{12} = E_{21} = E_{13} = E_{31} = 0$. Let the coordinate '$C$' be ($X_c$, Y_c) with respect to X and Y axes passing through any origin 'OR'. In Eq. (48b) substituting for x^* as

$$x^* = (X^* - X_c) \tag{52}$$

Then E_{12} may be written as

$$E_{12} = \int (A_{11}X^* + B_{11}\cos\beta)ds - X_c \int A_{11}ds = 0 \tag{53}$$

The X coordinate of 'C' may be written as

$$X_c = \frac{\bar{E}_{12}}{E_{11}} \tag{54}$$

where
Similarly Y coordinate of 'C' may be written as

$$Y_c = \frac{\bar{E}_{13}}{E_{11}} \tag{55}$$

If we take x, y axes as principal axes passing through 'C' (mechanical centroid) at an angle of η with respect to x axis such that

$$\tan 2\eta = \frac{2E_{23}}{(E_{22} - E_{33})} \tag{56}$$

then E_{22} and E_{33} calculated with respect to the principal axes become Principal mechanical moments of Inertia and $E_{23} = 0$.

7. Mechanical shear centre

E_{24} and E_{34} are made zero if the pole 'S' is selected at mechanical shear centre and x and y-axes passing through mechanical centroid.

The mechanical property E_{24} may be written as

$$E_{24} = \int (A_{11}\bar{\omega}x^* - B_{11}qx^* + B_{11}\bar{\omega}\cos\beta - D_{11}q\cos\beta)ds \tag{57}$$

where $\bar{\omega}$ is the sectorial coordinate or warping coordinate with 'S' as the pole and 'O' as the origin of the contour and is defined as (see Fig. 7)

$$\bar{\omega} = \bar{\omega}_c - e_x y^* + e_y x^* \tag{58}$$

where $\bar{\omega}_c$ is the warping coordinate with 'C' as the pole and 'O' as the origin for the contour and 'q' is written as

$$q = q_c + e_x \sin\beta - e_y \cos\beta \tag{59}$$

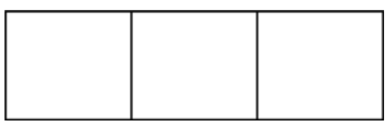

Fig. 7 Multi-cellular box girder

Hence E_{24} is written as

$$E_{24} = E_{24}^{c} - e_x E_{23}^{c} + e_y E_{22}^{c} = 0 \tag{60}$$

Similarly E_{34} is written as

$$E_{34} = E_{34}^{c} - e_x E_{33}^{c} + e_y E_{23}^{c} = 0 \tag{61}$$

Solving Eqs. (60) and (61), we get

$$e_x = \frac{\overline{E}_{34}^{c}}{\overline{E}_{33}^{c}}; \quad e_y = -\frac{\overline{E}_{24}^{c}}{\overline{E}_{22}^{c}} \tag{62}$$

where

$$\overline{E}_{22}^{c} = E_{22}^{c}\left(1 - \frac{E_{23}^{2}}{E_{22}^{c} E_{33}^{c}}\right) \tag{63a}$$

$$\overline{E}_{33}^{c} = E_{33}^{c}\left(1 - \frac{E_{23}^{2}}{E_{22}^{c} E_{33}^{c}}\right) \tag{63b}$$

and

$$\overline{E}_{24}^{c} = \overline{E}_{24}^{c} - \frac{E_{34}^{c}}{E_{33}^{c}} E_{23}^{c} \tag{64a}$$

$$\overline{E}_{34}^{c} = \overline{E}_{34}^{c} - \frac{E_{24}^{c}}{E_{22}^{c}} E_{23}^{c} \tag{64b}$$

By making mechanical shear centre as the pole, E_{24} and E_{34} are made zero. E_{14} may be made zero by selecting 'O' as mechanical sectorial centroid as

$$E_{14} = \int (A_{11}\overline{\omega} - B_{11} q)\, ds = 0 \tag{65}$$

where $\overline{\omega}$ is the normalized coordinate along the centre line of the contour. If it is not taken at sectorial centroid (say at any other point 'M')

$$\overline{\omega} = \overline{\omega}_M - \overline{\omega}_{OM} \tag{66a}$$

$$\overline{q} = q_M - q_{OM} \tag{66b}$$

Then E_{14} becomes

$$E_{14} = \int (A_{11}(\overline{\omega}_M - \overline{\omega}_{OM}) - B_{11}(q_M - q_{OM}))\, ds \tag{67}$$

Neglecting higher order term ($\int B_{11} q_{OM} ds$), we can obtain

$$\overline{\omega}_{OM} = \frac{E_{14}^{M}}{E_{11}} \tag{68}$$

Then normalized warping coordinate may be written as

$$\overline{\omega} = \overline{\omega}_M - \overline{\omega}_{OM} \tag{69}$$

$\overline{\omega}_{OM}$ enables one to calculate the sectorial centroid 'O' if any arbitrary point 'M' is known. $E_{j5}\ldots j = 1, 4$ are very small compared to other coefficients of E matrix and hence for all practical purposes if one selects 'C' as mechanical centroid, 'S' as mechanical shear centre and 'O' as mechanical sectorial centroid, the matrix [E] given in Eq. (47) is diagonal.

The normalised warping coordinate for open section is

$$\overline{\omega} = \omega^* \tag{70a}$$

and for closed section

$$\overline{\omega} = \omega^* + \int \psi ds \tag{70b}$$

Hence in general, the modified normalized warping coordinate for open and closed section may be written as

$$\overline{\omega} = \omega^* + \delta_c \int \psi ds \tag{71}$$

where δ_c is a tracer having a value of 0 or 1, depending on whether the cross section is open or closed.

From Eq. (21), ψ can be written as

$$\psi = \frac{1}{h\overline{G}_{sz}} \frac{\oint r^* ds}{\oint \frac{ds}{h\overline{G}_{sz}}} \tag{72}$$

where $\overline{G}_{sz}$ is defined as the effective inplane shear stiffness. The stiffness is defined as $N_{sz}/h\gamma_{sz}$ when the laminate is subjected to N_{sz} alone. But N_{sz} may be approximately be taken as

$$N_{sz} = A_{66}\gamma_{sz} \tag{73}$$

or

$$\overline{G}_{sz} = \frac{N_{sz}}{h\gamma_{sz}} = \frac{A_{66}}{h} \tag{74}$$

$$\overline{G}_{sz} h = A_{66} \tag{75}$$

Hence

$$\psi = \frac{1}{A_{66}} \frac{\oint r^* ds}{\oint \frac{ds}{A_{66}}} \tag{76}$$

Denoting ξ as

$$\xi = \frac{\oint r^* ds}{\oint \frac{ds}{A_{66}}} \tag{77a}$$

$$\text{or} \quad \psi = \frac{\xi}{A_{66}} \tag{77b}$$

In the expressions for E_{i5} (i = 1..5) the coefficients of δ_c must be calculated for each cell in a multi-cellular closed section. For example to calculate the coefficient of δ_c in E_{55} in Eq. (48)

$$\oint A_{66}\,\psi^2 ds = \frac{\oint r^* ds \oint r^* ds}{\oint \frac{ds}{A_{66}}} = \xi(\oint r^* ds) \tag{78}$$

To find ψ from Eq. (77a)

$$\xi = \left(\left(\oint \frac{ds}{A_{66}}\right)^{-1} \oint r^* ds\right) \tag{79a}$$

$$\psi = \frac{\xi}{A_{66}} \tag{79b}$$

For multi-cellular section, the indeterminate shear flow $\overline{N}_{sz}$ must be calculated by solving simultaneous equations.

Consider a three cell box section as shown in Fig. 7 to fine E_{55} the following procedure is adopted.

Find

$$b_{ii} = \oint_{cell\ i} \frac{ds}{A_{66}} \tag{80}$$

For common leg between cell i and j

$$b_{ij} = -\oint_{common\ member\ for\ i-j} \frac{ds}{A_{66}} \tag{81}$$

It can be seen that

$$\oint_{cell\ i} r^* ds = 2 \times Area\ of\ cell\ i = 2A_i \tag{82}$$

Hence ξ for each cell may be calculated from

$$\begin{Bmatrix} \xi_1 \\ \xi_2 \\ \xi_3 \end{Bmatrix} = \begin{bmatrix} b_{11} & b_{12} & b_{13} \\ b_{21} & b_{22} & b_{23} \\ b_{31} & b_{32} & b_{33} \end{bmatrix}^{-1} \begin{Bmatrix} 2A_1 \\ 2A_2 \\ 2A_3 \end{Bmatrix} \tag{83}$$

Then

$$\oint A_{66}\psi^2 ds = \langle 2A_1 \;\; 2A_2 \;\; 2A_3 \rangle \begin{Bmatrix} \xi_1 \\ \xi_2 \\ \xi_3 \end{Bmatrix} \tag{84}$$

8. Calculation of *A*, *B*, *D* matrices of lamina

A lamina may be composed of 'n' plies and the total thickness is given by (see Fig. 4)

$$h = \sum_{k=1}^{n} t_k \tag{85}$$

and

$$h_1 = -\frac{h}{2} \quad \text{for bottom surface}$$

$$h_2 = \frac{h}{2} \quad \text{for top surface} \tag{86}$$

In this paper, laminate consisting of symmetric, anti-symmetric and un-symmetric lamina has been used as shown in Fig. 8. For symmetric and anti-symmetric laminate it is enough if material, fibre orientation and thickness of laminates are specified for one half and other half is assumed as below.

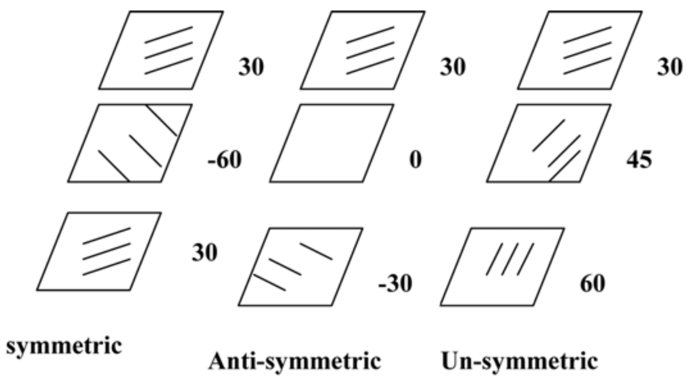

Fig. 8 Different types of laminates

8.1 Symmetric laminate

Fibre orientation in bottom half = Fibre orientation in top half
Thickness of laminates in bottom half = Thickness of laminates in top half
Material in bottom half = Material in top half

8.2 Anti-symmetric laminate

Fibre orientation in bottom half = Fibre orientation in top half
Thickness of laminates in bottom half = Thickness of laminates in top half
Material in bottom half = Material in top half

8.3 Unsymmetric laminate

Fibre orientation, thickness and material of each laminate are different from the other. The axial, coupled and bending stiffness matrices are calculated as given in Eq. (50).

9. Numerical evaluation of mechanical properties

The closed form integration for the computation of mechanical properties of any thin-walled open or closed composite cross section of a beam is difficult. Hence numerical integration using Gaussian quadrature is used.

Consider a cross section of a thin-walled beam as shown in Fig. 9 consisting of four elements and five nodes. Any one typical element is considered. Integration over the thickness direction has been carried out to find the axial, coupled and bending stiffnesses. Now integration has to be carried out along the length of the contour of the section. Consider the integral

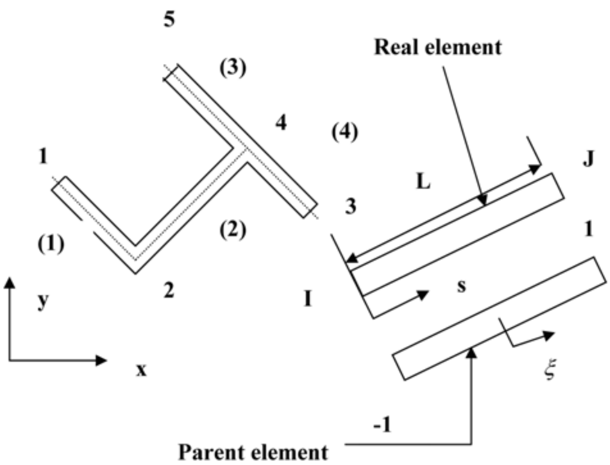

Fig. 9 Cross section of thin-walled beam

$$I = \int_0^L f(s)ds \tag{87}$$

To perform the numerical integration, 's' is written in terms of non-dimensional coordinate 'ς' as

$$s = \frac{L}{2}(1 + \varsigma) \tag{88}$$

Coordinate X may be written in terms of coordinates at the ends, using the shape functions as

$$x = \left\langle \frac{(1-\varsigma)}{2} \quad \frac{(1+\varsigma)}{2} \right\rangle \begin{Bmatrix} x_I \\ x_J \end{Bmatrix} \tag{89}$$

Similarly y, $\overline{\omega}$, $\cos\beta$, $\sin\beta$ are given at any point ς.

Applying three point Gaussian quadrature

$$I = \frac{L}{2}\sum_{i=1}^{3} H_i f_i \tag{90}$$

where

$$\begin{array}{lll} \varsigma_1 = -0.77459; & \varsigma_2 = 0.0; & \varsigma_3 = 0.77459 \\ H_1 = \frac{5}{9}; & H_2 = \frac{8}{9}; & H_3 = \frac{5}{9} \end{array} \tag{91}$$

Consider $f(s)$ is of the form "ABC". For calculation of mechanical properties of the section of curved beams $C = (1 - y/R)$ and for straight beams $C = 1$ $(R \rightarrow \infty)$.

To find the integral $\sum_{k=1}^{n} \int A_{11}^k x^{*2} ds = \sum_{k=1}^{n} A_{11}^k \int x^* x^* ds$

$$I = \int f(s)ds = \int A\ B\ C\ ds \text{ where } A = x^*;\ B = x^*;\ C = \frac{1}{(1 - y^*/R)} \tag{92}$$

Using the above procedure, all the mechanical properties given in Eq. (48) can be calculated. For straight beam R can be assumed as a high value.

10. Computer program

A computer program "FUNGEN.FOR" and "CLPROP.FOR" are developed in FORTRAN to find the mechanical properties of composite thin-walled beam of open or closed cross section. Before applying this program to composite beam examples, simple numerical examples of thin-walled sections of isotropic material are solved and compared with the available results

11. Numerical examples

Example 1. It is required to find the properties of thin-walled open mono-symmetric section as

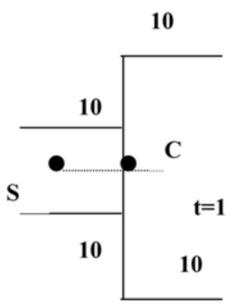

Fig. 10(a) Monosymmetric section

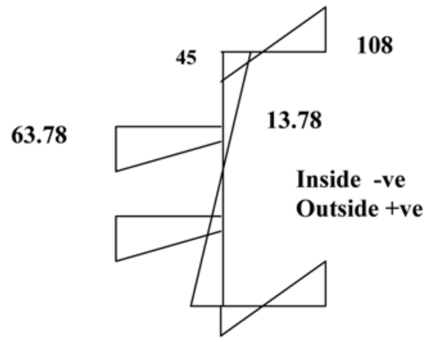

Fig. 10(b) Normalized warping coordinate

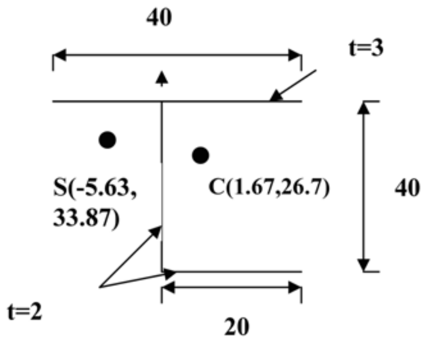

Fig. 11(a) Unsymmetric section

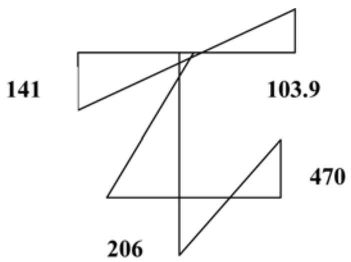

Fig. 11(b) Normalized warping

shown in Fig. 10(a). For isotropic sections $Q_{11} = Q_{22} = Q_{66} = 1$ and all other elements of Q matrix are zero. We arrive at St-Venant constant E_{55} = 23.33 and the sectorial moment of inertia as $E_{44} = I_\omega = 11.148 \times 10^4$. Centre of gravity C(0,15) and shear centre S(–2.788, 15) as shown in Fig. 10(a). Normalized warping coordinate diagram is shown in Fig. 10(b) and these values agree with the values calculated by different method. Since it is mono-symmetric section, shear centre lies on axis of symmetry, i.e., x axis.

Example 2. It is required to find the properties of unsymmetrical thin-walled open section as shown in Fig. 11(a). We arrive at St-Venant constant E_{55} = 519.94 (520[9]) and the sectorial moment of inertia as $E_{44} = I_\omega$ = 3912669(3914000[9]). Centre of gravity C(1.67,26.67) and shear centre S(–5.63,33.87) as shown in Fig. 11(a). Normalized warping coordinate diagram is shown in Fig. 11(b) and the properties agree with the published results of Murray (1984).

Example 3. Consider a crane girder (single cell) as shown in Fig. 12(a). We get the following properties as

Centroid = C(139.8,253.4)
Shear Centre = S(99.45,273.18)
E_{55} = 275309200 (275020000)[9]
$E_{44} = I_\omega = 43.49199 \times 10^9$ (43.65×10^9[9])

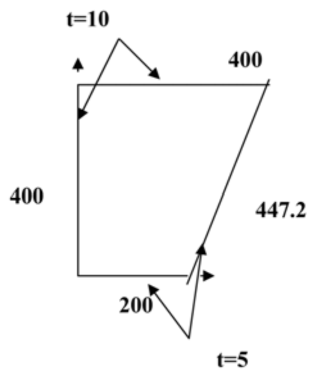

Fig. 12(a) Closed section

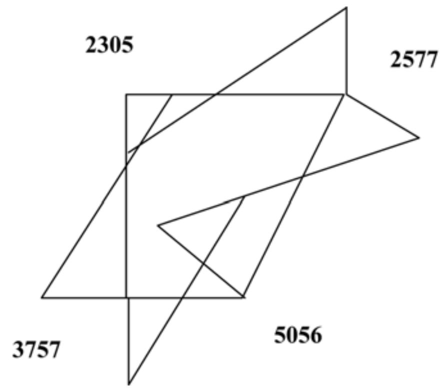

Fig. 12(b) Normalized warping

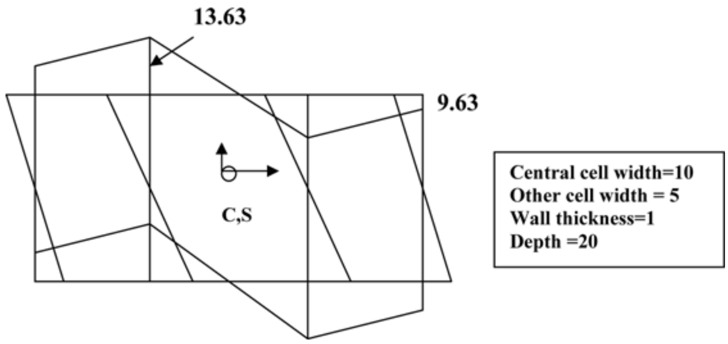

Fig. 13 Normalized warping

Normalized warping coordinate diagram is shown in Fig. 12(b) and the properties agree with the published results of Murray (1984).

Example 4. Consider a girder whose cross section is a three-cell box girder (see Murray 1984). Since the cross section is symmetric with respect to both x and y axes, the joint 1 is taken at any one of the point of symmetry as shown in Fig. 13. Hence joint 1 is assumed at the mid point of the top beam of middle cell so that the normalized warping is zero at that point. Simultaneous equations are solved to determine ξ and hence all the properties. The following properties are obtained as

$$E_{55} = 8767(8727)$$
$$E_{44} = I_{\omega} = 7437(7438)$$

C and S coincide as shown in Fig. 13. The bracketed values are from Murray (1984).

Example 5. Consider a thin-walled box girder with two cells (Connor 1976) as shown in Fig. 14(a). It is mono-symmetric with respect to x axis. The positions of Centre of gravity and shear centre viz:- $C(15.56,5)$; $S(16.11,5)$ agree with Connor (1976). The normalized warping diagram is shown in Fig. 14(b). If the section is unsymmetric, the sectorial centroid must be chosen randomly and should be found out by trial and error.

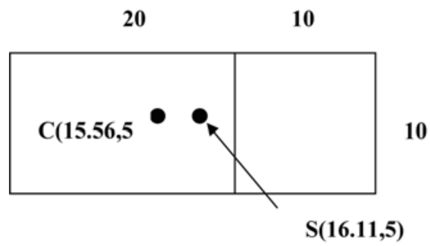

Fig. 14(a) Twin cell box girder (t = 1)

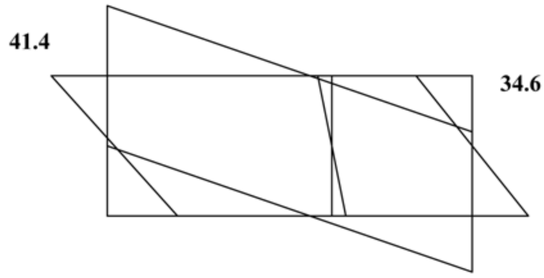

Fig. 14(b) Normalized warping

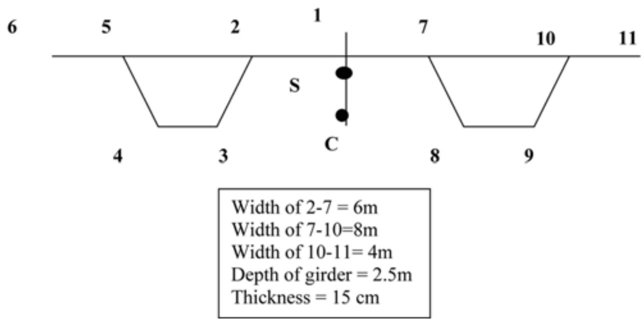

Fig. 15(a) Combination of open and closed section

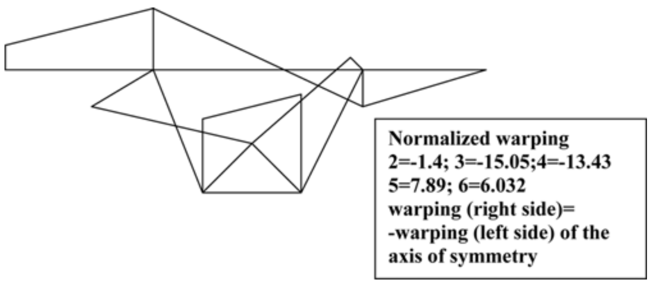

Fig. 15(b) Normalized warping

Example 6. Consider a thin-walled box girder whose profile is shown in Fig. 15(a). This is a combination of open and closed sections. Three members 6-4, 3-8, 9-11 of very small thickness are introduced and the given section is analysed as a box section with five cells. The positions of Centroid and Shear Centre viz:- $C(0,1.790)$ and $S(0,2.03)$. The results agree with Murray (1984). The normalized diagram is as shown in Fig. 15(b).

Example 7. Consider a three cell box girder as shown in Fig. 16(a). The positions of centroid and shear centre are obtained as $C(10,10.45)$ and $S(10,10)$ and the normalized diagram is shown in Fig. 16(b).

Example 8. A thin-walled composite beam with an open cross section (a channel (Lee 2000)) is considered (see Fig. 17) in order to investigate the effects of anisotropy and laminate stacking sequence on the location of centre of gravity and shear centre. The following engineering constants of the composite beam are used.

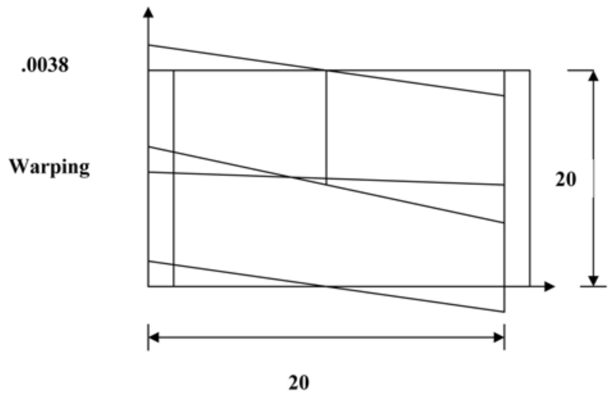

Fig. 16 3-Cell box girder

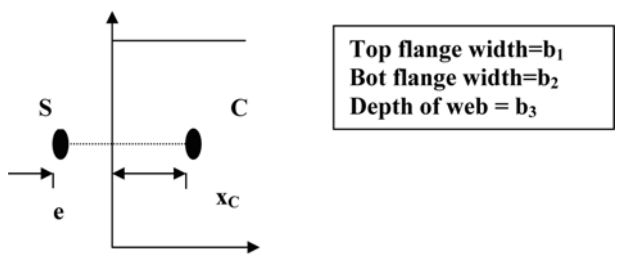

Fig. 17 Composite channel section

$$\frac{E_L}{E_T} = 40; \quad \frac{G_L}{E_T} = 0.6; \quad \gamma_{LT} = 0.25 \tag{93}$$

where L and T denote fibre directions and are perpendicular to fibre directions respectively. The geometry of the cross section is as follows.

$$t_1 = t_2 = t_3 = t$$

$$\frac{b_1}{t} = \frac{b_2}{t} = 20; \quad \frac{b_3}{t} = 40 \tag{94}$$

Hence the channel is mono-symmetric and hence the mechanical centre of gravity and mechanical shear centre will lie on x-axis. The fibre angle varies in two ways such as firstly angle ply laminate ($\pm\theta$) in the flanges and unidirectional fibre orientation in the web, secondly angle ply laminate ($\pm\theta$) in the web and unidirectional fibre orientation in the flanges. The location of centre of gravity 'C' and shear centre 'S' are illustrated in Fig. 18 with respect to fibre angle change. The classical isotropic solution corresponds to the case of fibre angle $\theta = 0$. When the mechanical centre of gravity moves towards centre and the mechanical shear centre moves away. The distance between mechanical shear centre and mechanical centre of gravity increases. As the fibre angle changes in the flanges, both mechanicanical centre of gravity and mechanical shear centre approach web contrary to the previous case. This example proves that the positions of mechanical centroid and mechanical shear centre are significantly affected by the laminate sequence.

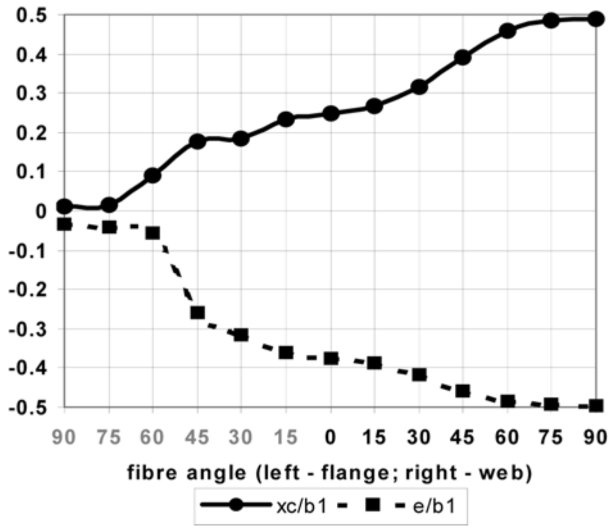

Fig. 18 Variation of positions of mechanical centroid and shear centre with respect to fibre orientations (Example 8)

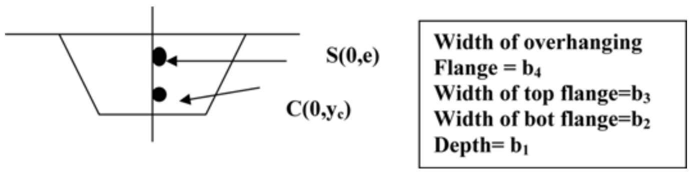

Fig. 19 Composite box girder

Example 9. A thin-walled composite beam with the combination of closed and open section is shown in Fig. 19 with (b_1/t = 20; b_2/t = 30; b_3/t = 40; b_4/t = 10). Similar to example 8 fibre angle varies in two ways. The locations of mechanical centroid and mechanical shear centre are shown in Fig. 20 with respect to fibre angle change. The mechanical centroid distance is more or less constant with y_c/b_1 = 0.6 whereas e/b_1 is at minimum at 0.4 with the fibre angle in the flange at 45 degrees (+ or – 45 degrees) and maximum at e/b_1 = 0.55 when the web angle is kept at 45 degrees (+ or –45 degrees).

Example 10. The object of this example is to design E_{33} (in the case of composite section) with maximum bending stiffness, which would be required, if the beam is to experience predominantly transverse loading. Already Savic *et al.* (2001) have solved the optimization problem of composite beams. An example of composite beam with dimensions 50.8 × 50.8 mm and double geometrical symmetry is considered in this study with material system of intermediate modulus graphite epoxy with E_{LL} = 158 Gpa; E_{TT} = 7.8 Gpa, G_{LT} = 4.75 MPa and γ_{LT} = 0.33 with ply thickness of 0.127 mm as shown in Fig. 21. The number of plies in each wall has been fixed and set to four and hence total thickness of flange and web laminate is 0.508 mm. The following convention for describing the laminate stacking sequence for an *I* section is adopted. The stacking sequence of the bottom flange is denoted first following the web and top flange. Always they are denoted from bottom to top for each flange and in the web from left to right. Fig. 22 shows the variation of E_{33} (bending

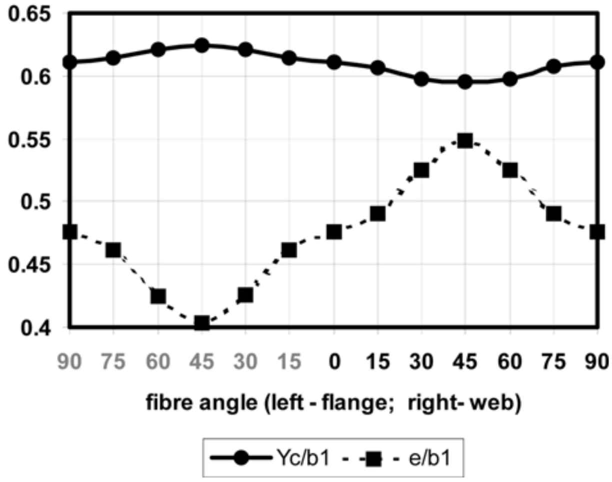

Fig. 20 Variation of positions of mechanical centroid and shear centre with respect to fibre orientations (Example 9)

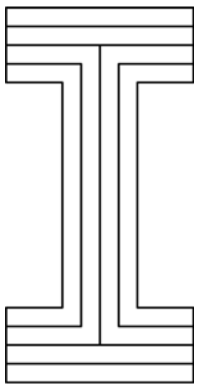

Fig. 21 Composite I beam. $[\theta_2/\theta_1/90/0]_T$-top flange, $[0/90]_s$-web, $[0/90/\theta_1/\theta_2]$-bot flange

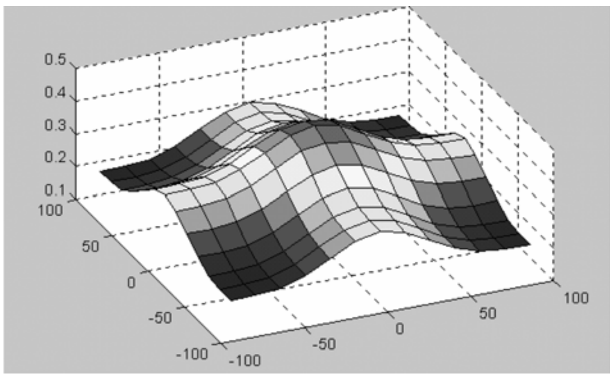

Fig. 22 Variation of $E_{33}/10^{10}$ for Example 10

Table 1 ($E_{33}/10^{10}$) for the composite beam (Example 10)

θ_2/θ_1	0	15	30	45	60	75	90
0	0.449	0.4336	0.395	0.3569	0.332	0.3247	0.3237
15	0.436	0.4178	0.3799	0.3411	0.3171	0.3089	0.307
30	0.395	0.379	0.3421	0.303	0.2792	0.271	0.27
45	0.3569	0.3411	0.303	0.264	0.24	0.232	0.2352
60	0.3329	0.3171	0.2792	0.24	0.216	0.208	0.2072
75	0.3247	0.3081	0.271	0.232	0.208	0.2	0.199
90	0.3237	0.307	0.270	0.2312	0.2072	0.199	0.198

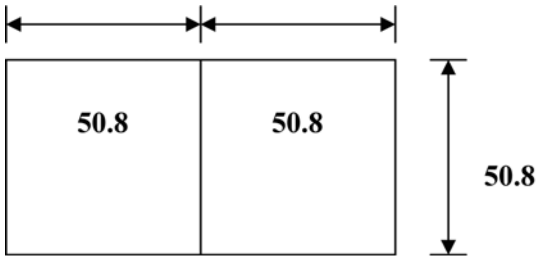

Fig. 23 Twin cell box girder

stiffness) (see Table 1) with respect to the orientation of θ_1 and θ_2 and it is seen E_{33} is maximum when the two angles are zero.

Example 11. The object of this example is to design a thin-walled box girder for maximum torsional stiffness which will be required if the beam is to experience predominant torsional bending loads. Again the box section of 101.6 × 50.8 mm is considered as shown in Fig. 23. In this study, material system of High performance Graphite/epoxy is considered with properties of E_{LL} = 470 Gpa; E_{TT} = 6.2 Gpa, G_{LT} = 5.58 MPa and γ_{LT} = 0.31, ply thickness = 0.127 mm. The number of plies in extreme webs is two and for all other flanges and web it is four. The following laminate sequence is adopted.

$$\text{Top flange} = [\theta_1/\theta_2]_{AS}$$
$$\text{Bottom flange} = [-\theta_1/-\theta_2]_{AS}$$
$$\text{Extreme webs} = [\theta_1/\theta_2]_{T}$$
$$\text{Middle web} = [\theta_1/\theta_2]_{SY}$$

Fig. 24 shows the variation of mechanical St.Venant constant E_{55} with respect to both the angles and it is seen that E_{55} is maximum = 10.49×10^{15} when both the angles are equal to 45 degrees. The values of E_{44} and E_{55} are given in Table 2.

Fig. 25 shows the variation of mechanical sectorial moment of Inertia E_{44} with respect to both the angles and it is seen that E_{44} is maximum when θ = 0; θ_2 = 30° to give value of E_{44} as 1.94×10^{10}.

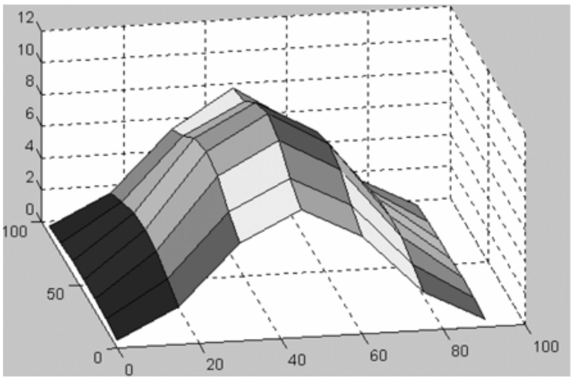

Fig. 24 Variation of $E_{55}/10^{15}$ for Example 11

Table 2 $(E_{55}/10^{15})/(E_{44}/10^{11})$ for the composite beam (Example 11)

θ_2/θ_1	0	15	30	45	60	75	90
0	0.495 33.6	2.41 1.6	6.17 0.2	8.05 0.095	6.17 0.13	2.41 0.8	0.495 15.2
15	0.65 161	2.996 29.4	6.94 5.3	8.85 2.53	6.94 3.2	2.996 13.5	0.65 67.7
30	0.702 194	3.53 73	7.99 19.3	10.04 9.3	7.99 10.0	3.53 26.3	0.702 62.9
45	0.711 171	3.67 74.2	8.37 20.8	10.49 9	8.37 7.8	3.67 15.9	0.711 31.9
60	0.702 141	3.53 51.6	7.99 11.9	10.04 4.2	7.99 2.7	3.53 4.6	0.702 10.3
75	0.65 96.2	2.996 16.6	6.94 2.4	8.85 0.74	6.94 0.4	2.99 0.65	0.605 2.73
90	0.495 18.9	2.41 0.86	6.17 0.05	8.55 0.024	6.17 0.013	2.41 0.029	0.495 0.44

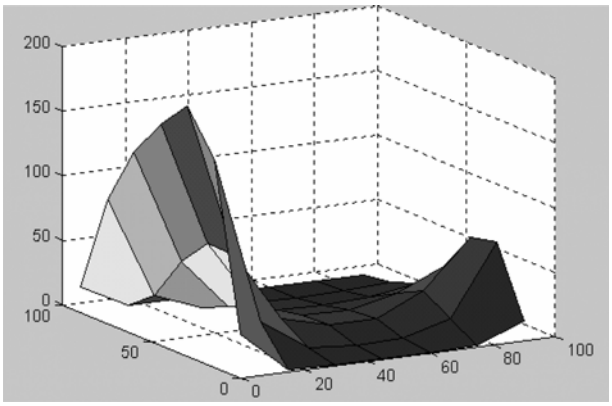

Fig. 25 Variation of $E_{44}/10^{11}$ for Example 11

12. Conclusions

A rigorous definition of mechanical centre of gravity, mechanical shear centre and mechanical sectorial centroid and other mechanical properties for a thin-walled composite beam with open/(or/ and) closed section. The method is applicable to any arbitrary laminate stacking sequence such as symmetric/anti-symmetric/un-symmetric and generic cross sectional shape. The program "FUNGEN" calculates the axial, bending and coupled matrices and the program "CLPROP" computes the sectional properties. First of all the program is applied to isotropic section and the properties are compared with published results. It is shown that the locations of mechnical centre of gravity and mechanical shear centre are generally dependent on fibre angle changes in the flanges and webs.

Two different examples are presented to illustrate the optimization process. In the first case, the objective is to maximize the beam bending stiffness for a composite *I* section and in the second case, the objective is to maximize beam St-Venant Torsional stiffness and warping stiffness for a composite thin walled closed section. In the first case, intermediate modulus/graphite epoxy system and in the second case high performance/graphite epoxy are considered. More general types of optimization of cross sections with constraints using Evolution Strategies will be discussed in another paper.

Acknowledgements

The author thanks the management and the Principal Dr. R. Rudramoorthy and Dr. J.V. Ramasamy, Head of Civil Engineering of PSG College of Technology for providing necessary facilities in carrying out the research work reported in this paper.

References

Bauld, N.R., Tzeng, L.S. and Vlasov, A. (1984), "Theory for fibre reinforced beams with thin-walled open cross section", *Int. J. Solids Struct.*, **20**(3), 277-297.

Bhaskar, K. and Librescu, L.A. (1995), "Geometrically non-linear theory for laminated anisotropic thin-walled beams", *Int. J. Eng. Sci.*, **33**(9), 1331-1344.

Chen, W.F. and Atsuta, T. (1977), *Theory of Beam-Columns – Vol. 2- Space Behaviour and Design*, N.Y., McGraw-Hill.

Connor, J.J. (1976), *Analysis of Structural Member Systems*, The Ronald Press Co., NY.

Gjelsvik, A. (1981), *The Theory of Thin-Walled Bars*, New York, Wiley.

Kaw, A.K. (1997), *Mechanics of Composite Materials*, CRC Press, USA.

Lee, J. (2001), "Centre of gravity and shear centre of thin-walled open cross section composite beams", *Comp. Struct.*, **52**, 255-260.

Murray, D.W. and Rajasekaran, S. (1975), "A technique for formulating beam equations", *J. Eng. Mech.*, ASCE, **101**, No. EM5, Proc. Paper 11613, Oct., 561-573.

Murray, N.W. (1984), *Introduction to the Theory of Thin-Walled Structures*, Clarendon Press, Oxford.

Rajasekaran, S. (1994), "Equations for tapered thin-walled beams of generic open section", *J. Eng. Mech.*, ASCE, **120**(8), 1607-1629.

Rajasekaran, S. and Padmanabhan, S. (1989), "Equations for curved beams", *J. Eng. Mech.*, ASCE, **115**(5), 1094-1111.

Savic, V., Tuttle, M.E. and Zabinsky, Z.B. (2001), "Optimization of composite I-sections using fibre angles as

design variables", *Comp. Struct.*, **53**, 265-277.
Taufik, A., Barrace, J.J. and Lorin, F. (1999), "Composite beam analysis with arbitrary cross section", *Comp. Struct.*, **44**, 189-194.
Vlasov, V.Z. (1961), *Thin Walled Elastic Beams*, 2nd Ed., Israel Program for Scientific Translation. Jerusalem, Israel, 1961.
Wagner, W. and Gruttmann, F. (2002), "A displacement method for the analysis of flexural shear stresses in thin-walled isotropic composite beams", *Comput. Struct.*, **80**, 1843-1851.
Wu, X.X. and Sun, C.T. (1992), "Simplified theory for composite Thin-walled beams", *AIAA J.*, **30**(12), Dec., 2945-2951.